

## New Dynamical Scaling Universality for Quantum Networks Across Adiabatic Quantum Phase Transitions

O. L. Acevedo,<sup>1</sup> L. Quiroga,<sup>1</sup> F. J. Rodríguez,<sup>1</sup> and N. F. Johnson<sup>2</sup>

<sup>1</sup>*Departamento de Física, Universidad de los Andes, A.A. 4976, Bogotá, Colombia*

<sup>2</sup>*Department of Physics, University of Miami, Coral Gables, Miami, Florida 33124, USA*

(Received 19 September 2013; revised manuscript received 22 November 2013; published 22 January 2014)

We reveal universal dynamical scaling behavior across adiabatic quantum phase transitions in networks ranging from traditional spatial systems (Ising model) to fully connected ones (Dicke and Lipkin-Meshkov-Glick models). Our findings, which lie beyond traditional critical exponent analysis and adiabatic perturbation approximations, are applicable even where excitations have not yet stabilized and, hence, provide a time-resolved understanding of quantum phase transitions encompassing a wide range of adiabatic regimes. We show explicitly that even though two systems may traditionally belong to the same universality class, they can have very different adiabatic evolutions. This implies that more stringent conditions need to be imposed than at present, both for quantum simulations where one system is used to simulate the other and for adiabatic quantum computing schemes.

DOI: [10.1103/PhysRevLett.112.030403](https://doi.org/10.1103/PhysRevLett.112.030403)

PACS numbers: 05.30.Rt, 64.60.an, 64.60.Ht

Scaling is ubiquitous in nature, with critical exponents being used to characterize universal phase transition phenomena in both equilibrium and nonequilibrium systems [1]. Scaling functions go beyond critical exponents by incorporating richer information about the dynamics of the underlying many-body system, including finite-size effects, and hence extending the range of validity over which theoretical predictions can describe empirical data [2]. In the field of critical phenomena, much attention has recently been directed to adiabatic quantum phase transitions (QPTs). In addition to their fundamental role as zero-temperature many-body quantum phenomena [3], QPTs represent a key ingredient of current quantum computation schemes [4,5].

Recent studies show that as a QPT phase boundary is crossed slowly in models with finitely connected lattices [6–11], the short-range interaction allows a correlation length to be defined and, hence, scaling to be examined through the Kibble-Zurek mechanism (KZM) [6,12]. However, an implicit limiting assumption of the KZM is that adiabatic evolution holds except for a small threshold around the critical point, during which spatial defects in the order parameter are created and power-law relations emerge, defined by critical exponents. For slower quench rates, adiabatic perturbation theory (APT) can be invoked instead and excitations predicted in terms of quasiparticles [9,13]. However, totally connected lattice models such as the Dicke model (DM) and the Lipkin-Meshkov-Glick model (LMGM) [14] have no spatial order parameter and, hence, lack a clear connection to existing theories such as KZM. This may explain the lack of general results to date for the adiabatic QPT regime, with the exception of bosonic excitation estimates in the DM using simplifying mean-field and rotating wave approximations [15], scaling of

final excitations in the LMGM [16], and dynamical characterizations of the QPT through a monochromatic modulation of the annealing parameter [17].

In a QPT, critical exponents are extracted from the power-law behavior in the thermodynamic limit (TL), of equilibrium quantities such as energy gaps and susceptibilities around the quantum critical point (QCP) [6]. However, when finite-size scaling is considered, continuous functions emerge at the phase boundary. Here we show that, contrary to common belief, these critical functions—but not critical exponents—provide a unified description of QPT dynamics, as encoded by nonadiabatic indicators such as heating and ground-state fidelity. Furthermore, they encompass both finite-range [e.g., transverse field Ising model (TFIM)] and fully connected systems (e.g., DM and LMGM [18]) and, hence, overcome the limitations of KZM and APT. In addition to applications in adiabatic quantum computing [4,5], QPTs have been experimentally realized using ultracold atomic systems [19,20]. By revealing continuous-time details of the size-independent dynamical behavior of quantum many-body systems, our analysis goes beyond critical exponent analyses such as KZM and connects to studies of avalanchelike events across classical phase boundaries [2]. KZM-like and an APT-like regime are both naturally incorporated in and illuminated by this new framework. We find that the traditional universality of critical exponents is insufficient to describe the analogous dynamical evolutions of different models, thereby casting doubt on an implicit assumption of quantum simulations [21] in which particular models are taken to act as experimental surrogates of each other.

We focus on three models for which experimental realizations exist or have been proposed [22]. Each features  $N$  qubits with differing interaction connectivities

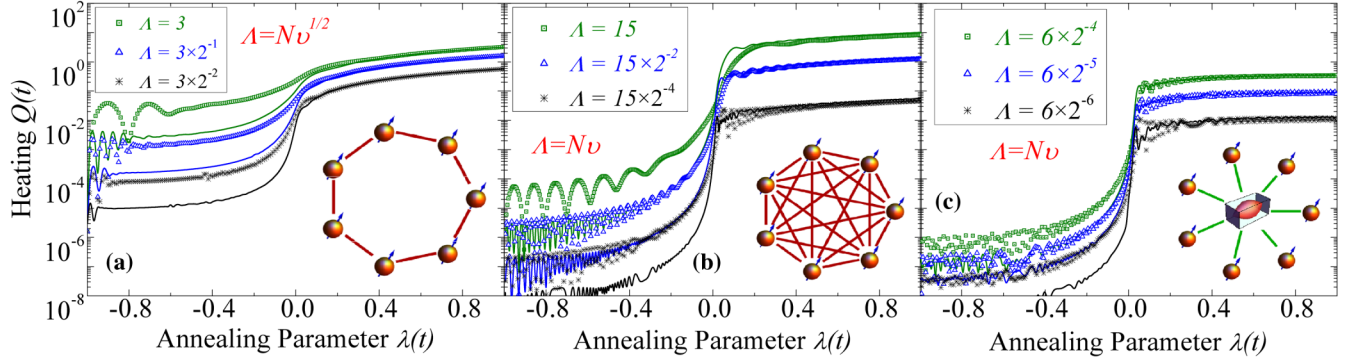


FIG. 1 (color online). Time evolution of heating  $Q(t)$  for (a) TFIM, (b) LMGM, and (c) DM. Insets show how the qubits interact in these three models. In each panel, we present results for three different scaled annealing velocities  $\Lambda$  (different colors) and two system sizes: TFIM, continuous lines ( $N = 160$ ) and symbols ( $N = 80$ ); LMGM, continuous lines ( $N = 2^{11}$ ) and symbols ( $N = 2^9$ ); DM, continuous lines ( $N = 2^9$ ) and symbols ( $N = 2^8$ ). Notice that for well inside the ordered phase ( $\lambda > 0$ ) for arbitrarily connected models, curves with the same  $\Lambda$  but different size  $N$  collapse.

(Fig. 1 insets). The following generic, dimensionless, time-dependent Hamiltonian ( $\hbar = 1$ ) describes the TFIM and LMGM:

$$\hat{H}(t) = -\sum_{i=1}^N \hat{\sigma}_z^{(i)} - \frac{\lambda(t) + 1}{N^s} \sum_{\langle i,j \rangle} \hat{\sigma}_x^{(i)} \hat{\sigma}_x^{(j)}, \quad (1)$$

where  $\{\hat{\sigma}\}$  are Pauli matrices and  $\langle i, j \rangle$  denotes pairs of interacting qubits. We choose the interaction strength  $\lambda(t)$  as the annealing parameter. In the TFIM, only pairs of nearest neighbors in a circular lattice interact, whereas in the LMGM all pair interactions are present. At  $\lambda = 0$  in the TL, the system is at the QCP [3,23], where a minimum-value energy gap arises between the ground state and the first excited accessible state.  $N^s$  in the denominator normalizes the interaction parameter according to size for the LMGM;  $s = 0$  in the TFIM, while  $s = 1$  in the LMGM. Like the LMGM, the DM has a totally connected lattice, but the qubit-qubit interaction is mediated by a boson mode: when the qubits and boson mode are in resonance, the Hamiltonian becomes

$$\hat{H}(t) = \sum_{i=1}^N \hat{\sigma}_z^{(i)} + \hat{a}^\dagger \hat{a} + \frac{\lambda(t) + 1}{2\sqrt{N}} (\hat{a}^\dagger + \hat{a}) \sum_{i=1}^N \hat{\sigma}_x^{(i)} \quad (2)$$

where  $\hat{a}^\dagger$  ( $\hat{a}$ ) is the mode's creation (annihilation) operator. The QCP in the TL is also at  $\lambda = 0$  [24].

To describe the crossing of the QPT, we show a simple case in which the annealing parameter evolves linearly as  $\lambda(t) = vt$  since it leads to relatively simple formulas, though we stress that extension to any power-law time dependence is straightforward (Supplemental Material [25]). We start in the ground state  $|\varphi_0(t_i)\rangle$  with  $\lambda(t_i) = -1$  at “negative” time  $t_i = -v^{-1}$  [i.e., the zero of time is defined as the instance where the system passes through  $\lambda(t_i) = 0$ ]. The systems in Eqs. (1) and (2) evolve with a

time-dependent state  $|\Psi(t)\rangle$  across the QCP, until positive time  $t_f$  where  $\lambda(t_f) = 1$ . For slow enough quench, the system should end in a final ground state  $|\varphi_0(\lambda(t_f))\rangle$  representing perfect adiabatic evolution. However, the QCP hinders the many-body system from achieving this result, since the minimal energy gap makes it easy for the system to jump out of the ground state. Because this gap gets smaller as the system size increases, ever slower quenches are necessary to keep the system in the ground state. Hence, the fundamental effect of the crossing of QPTs is the loss of adiabatic evolution. We employ two indicators to probe this result: (1) Ground-state fidelity  $p_0(t) = |\langle \varphi_0(t) | \Psi(t) \rangle|^2$  measuring the overlap between the actual dynamical state  $|\Psi(t)\rangle$  and  $|\varphi_0(t)\rangle$ . It lies in the interval  $0 \leq p_0 \leq 1$  and has its maximum value for perfect adiabatic evolution. (2) Heating  $Q(t) = \langle \Psi(t) | \hat{H}(t) | \Psi(t) \rangle - E_0(t)$ , which is always non-negative, and for adiabatic evolution is zero [26]. [ $E_0(t)$  is the instantaneous ground-state energy]. Details of the calculation are shown in the Supplemental Material [25].

Figure 1 shows the heating  $Q(t)$  for  $\lambda \in [-1, 1]$ . For  $\lambda < 0$ , the behavior at a given  $v$  is independent of size, with virtually no loss of adiabaticity provided  $v$  is small enough [13]. The stronger heating behavior that emerges above the QCP results from excitations forming, following a scaled velocity  $\Lambda$ . The almost vertical step around  $\lambda = 0$  shows that the evolution is essentially adiabatic, except for the narrow interval around the QCP where the major excitations are formed. Since the important aspects of the quenching are defined around the QCP, we analyze the system's state in terms of instantaneous eigenstates

$$|\Psi(t)\rangle = \sum_{n=0} a_n(t) e^{-i \int_{t_0}^t E_n(t') dt'} |\varphi_{\lambda(t)}^{(n)}\rangle, \quad (3)$$

where  $\hat{H}(t) |\varphi_{\lambda(t)}^{(n)}\rangle = E_n(\lambda(t)) |\varphi_{\lambda(t)}^{(n)}\rangle$  for every time  $t$ . The  $a_n(t)$  evolution follows

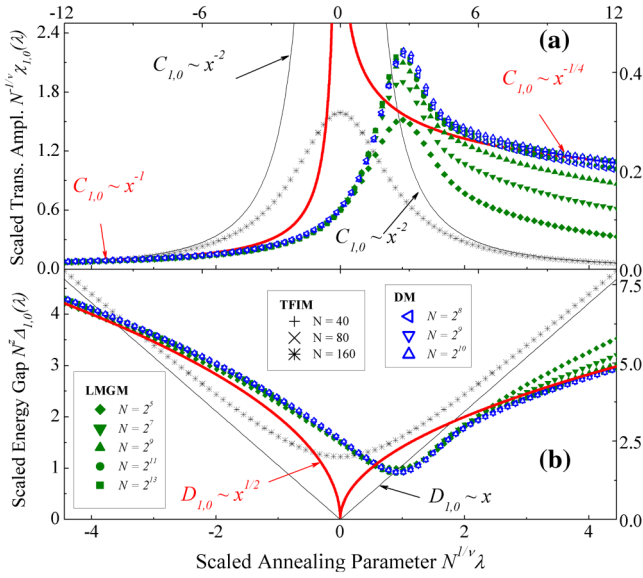


FIG. 2 (color online). Universal behavior of finite-size critical functions (a)  $C_{1,0}$  and (b)  $D_{1,0}$  as defined in Eqs. (5) and (6). Symbols show results for system size  $N$  while continuous curves are power-law predictions in the TL. (Thick red line is for both DM and LMGM. Thin black line is for TFIM). Scales for the DM and LMGM are given at the left bottom and right top, respectively, and show that the critical functions for both models have the same shape since they belong to the same universality class. Horizontal scale for the TFIM is at the top, while the vertical scale is not present but goes up to 25 in (a) and 0.25 in (b).

$$\frac{da_n(\lambda)}{d\lambda} = \sum_{m \neq n} e^{i\nu^{-1}\phi_{n,m}^{(N)}(\lambda)} \chi_{n,m}^{(N)}(\lambda) a_m(\lambda), \quad (4)$$

where  $\phi_{n,m}^{(N)}(\lambda) \equiv \int_0^\lambda \Delta_{n,m}^{(N)}(\lambda') d\lambda'$ , which is the integral of the energy gap between eigenstates  $n$  and  $m$ . The transition amplitudes  $\chi_{n,m}^{(N)} \equiv -\langle \varphi_\lambda^{(n)} | \frac{d}{d\lambda} (|\varphi_\lambda^{(m)}\rangle) \rangle$  can be written as  $\chi_{n,m}^{(N)}(\lambda) = [V_{n,m}^{(N)}(\lambda)] / [\Delta_{n,m}^{(N)}(\lambda)]$  whenever eigenstates  $n$  and  $m$  are nondegenerate, and  $V_{n,m}^{(N)}$  are the matrix elements of the interaction part of the Hamiltonian, mediated by  $\lambda$ . The superscript  $(N)$  indicates that all the functions depend on the system size. Equation (4) is usually the central part of the adiabatic theorem [27], which states that if  $v \ll |\Delta_{n,m}/\chi_{n,m}|$ , then  $\{a_n\}$  remain constant. For sufficiently slow annealing, this is satisfied outside the QCP region, implying that only the eigenstates that reach a zero gap in the TL are relevant for the loss of adiabaticity. It is at this point that dynamical critical functions enter the picture, since  $\chi_{n,m}$  and  $\Delta_{n,m}$  obey a scaling relation when  $|\lambda| \ll 1$  [9,23,28]

$$\chi_{n,m}^{(N)}(\lambda) = N^{1/\nu} C_{n,m}(x), \quad (5)$$

$$\Delta_{n,m}^{(N)}(\lambda) = N^{-z} D_{n,m}(x), \quad (6)$$

where  $x \equiv N^{1/\nu} \lambda$  with  $\nu$  and  $z$  determined through the power-law behavior in the TL [24,3]. Figures 2(a) and 2(b) present these critical functions between the ground and first-excited states and show how they start matching the TL power-law behavior for sufficiently large  $N$  and  $x$ . It follows that  $\nu = z = 1$  for the TFIM and  $\nu = 3/2$  and  $z = 1/3$  for DM and LMGM [3,29].

Our main result is that the evolution in Eq. (4) can now be cast in size-independent form

$$\frac{da_n(x)}{dx} = \sum_{m \neq n} e^{i\Lambda^{-1/\mu}\Phi_{n,m}(x)} a_m(x) C_{n,m}(x), \quad (7)$$

where the scaled velocity  $\Lambda = Nv^\mu$ , the dynamical phase difference  $\Phi_{n,m}(x) = \int_0^x D_{n,m}(x') dx'$ , and  $\mu = \nu/(1+z\nu)$ . Equation (7) predicts universal results in terms of excitation probabilities  $p_n \equiv |a_n|^2$  and the ground-state fidelity. Since the energy spectrum has a regular behavior, the heating will also be universal since  $Q \equiv \sum_n p_n \Delta_{n,0}$ . This prediction is confirmed in Fig. 3 with both adiabatic quantifiers behaving in a size-independent manner across the critical region. We note that the collapse only occurs during and after the critical threshold, because it is around the QCP that the adiabatic indicators are significantly affected, and it is in this region that universal functions exist. Once the QCP is passed ( $\lambda > 0$  stage), the evolution is again essentially adiabatic and the accumulated nonadiabatic effects of crossing the critical threshold remain dominant, clamping the subsequent collapsed evolution. Therefore, our results show that by generalizing from critical exponents to critical functions, we expand the traditional description focused on scaling at a fixed final value of  $\lambda$  as in Fig. 1, to a complete temporal collapse picture as shown in Fig. 3 around the QCP.

This new picture includes well-known results predicted by KZM and APT as special cases, since both can be expressed as power-law dependencies at the end of the quenching process [16]. In the lower velocity APT regime where there is low probability of leaving the ground state, the following approximation holds for  $n \neq 0$ :

$$a_n(\lambda) \approx \int_{-1}^\lambda e^{i\nu^{-1}\phi_{n,0}(\lambda')} \chi_{n,0}(\lambda') d\lambda'. \quad (8)$$

Since the integrand is only non-negligible around the QCP, it follows that  $|a_n| \sim v$ , for which  $p_n \sim v^2$  and, hence,  $Q_f \sim v^2$ . The higher velocity KZM regime is characterized by excitations being large enough to discard APT, replacing it by an adiabatic-impulse-adiabatic approximation in which the size of the threshold at which major excitations are created is defined by a definite time  $t_K$  or, equivalently, a critical value of  $x_K = vN^{1/\nu} t_K$ .

In the traditional KZM, as is the case of the TFIM, a healing time has been directly related to the inverse energy gap [6], making  $t_K \Delta(t_K) = t_k (vt_K)^{\nu z} \sim 1$  and then

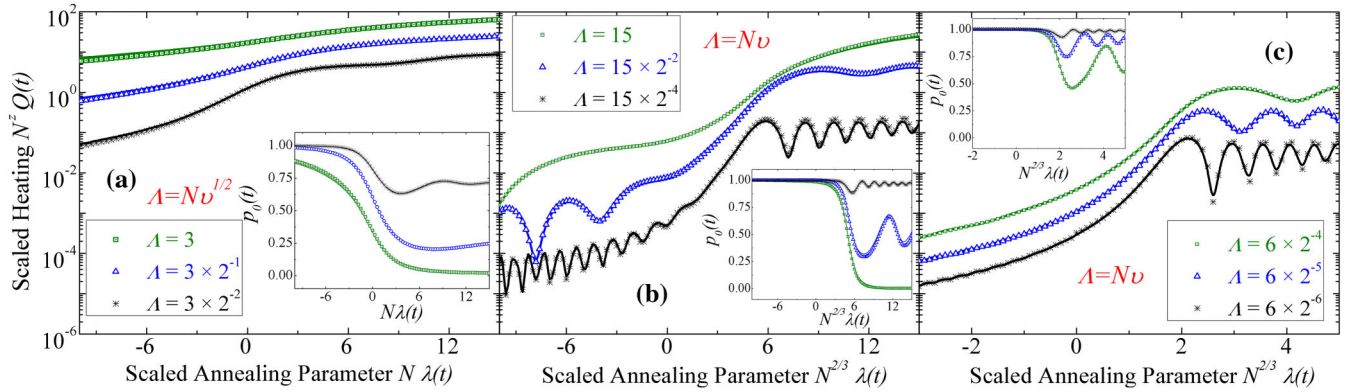


FIG. 3 (color online). Magnification and rescaling of the results in Fig. 1 around QCP, as described by Eq. (7). Collapse is no longer restricted to a nearly constant value well after the QCP. Instead, a continuous-in-time, size-independent behavior is revealed, a prediction that lies outside the scope of critical exponent analysis. Insets show continuous scaling also present for the ground-state fidelity  $p_0(t)$ . Exponent  $z = 1$  for the TFIM, whereas  $z = 1/3$  for both LMGM and DM.

$x_K \sim \Lambda^{1/\nu}$ . With this estimate, an adiabatic indicator such as heating can be predicted through  $Q_f \sim D(x_K) \sim \Lambda^z$ . For the TFIM ( $z = 1$ ), this KZM prediction has been confirmed [7]. By stark contrast, totally connected models do not match this estimate: instead of an exponent  $1/3$ , a scaling  $Q_f \sim \Lambda^{3/2}$  has been found [16]. However, Fig. 2(a) reveals that in the  $\lambda > 0$  phase, there is an anomalous  $x^{-1/4}$  dependence caused by a divergent  $\chi \sim N^{1/2}$  transition amplitude [29]. Furthermore, in the  $\lambda < 0$  phase, an  $x^{-1}$  dependence is present. Such exponents are specific to infinite dimensional lattices such as the LMGM and DM, and this difference is not taken into account in the KZM.

The failure of the KZM prediction for LMGM and DM highlights the accuracy of a dynamical function approach as compared to power-law relations based on critical exponents. Dynamical critical functions provide a full time-resolved picture of dynamical scaling in the near-adiabatic regime, even around the critical threshold where excitations have not yet stabilized—hence, understanding their properties is crucial for the design and cross-checking of annealing schemes in quantum simulations. The fact that the curves for LMGM and DM in Figs. 2(a) and 2(b) have essentially the same shape might erroneously be taken as sufficient justification for using one as a quantum simulation of the other—however, this is not true. No matter how a dynamical curve in Fig. 3(b) is scaled, its shape will never completely match any curve of Fig. 3(c). Instead, a thorough examination of Eq. (7) reveals that equivalence between both near-adiabatic evolutions can only be achieved if the functions  $\{C_{n,m}(x)\}$  scale as  $C_{n,m}^{\text{DM}}(\alpha x) = \alpha^{-1} C_{n,m}^{\text{LMGM}}(x)$ , which is a stringent condition that is undetectable through critical exponent analysis. In short, although equilibrium equivalence between systems around the QCP can be accomplished just by having identical critical exponents, achieving *dynamical* equivalence requires further tuning of model parameters, thereby

partitioning the traditionally static universality classes into *subsets* of dynamically equivalent systems.

The authors thank Ana Maria Rey for a critical reading of the manuscript. O. L. A., L. Q., and F. J. R. acknowledge financial support from Proyectos Semilla-Facultad de Ciencias at Universidad de los Andes and project “Quantum control of non-equilibrium hybrid systems,” UniAndes. O. L. A. acknowledges financial support from Colciencias, Convocatoria 511.

- [1] H. E. Stanley, *Rev. Mod. Phys.* **71**, S358 (1999).
- [2] S. Papanikolaou, F. Bohn, R. L. Sommer, G. Durin, S. Zapperi, and J. P. Sethna, *Nat. Phys.* **7**, 316 (2011).
- [3] S. Sachdev, *Quantum Phase Transitions* (Cambridge University Press, Cambridge, England, 2011).
- [4] E. Farhi, J. Goldstone, S. Gutmann, J. Lapan, A. Lundgren, and D. Preda, *Science* **292**, 472 (2001); R. Schützhold and G. Schaller, *Phys. Rev. A* **74**, 060304 (2006).
- [5] S. Boixo, T. F. Rønnow, S. V. Isakov, Z. Wang, D. Wecker, D. A. Lidar, J. M. Martinis, and M. Troyer, *arXiv:1304.4595*; S. Santra, G. Quiroz, G. V. Steeg, and D. Lidar, *arXiv:1307.3931*.
- [6] J. Dziarmaga, *Adv. Phys.* **59**, 1063 (2010).
- [7] W. H. Zurek, U. Dorner, and P. Zoller, *Phys. Rev. Lett.* **95**, 105701 (2005); L. Cincio, J. Dziarmaga, M. M. Rams, and W. H. Zurek, *Phys. Rev. A* **75**, 052321 (2007).
- [8] F. M. Cucchietti, B. Damski, J. Dziarmaga, and W. H. Zurek, *Phys. Rev. A* **75**, 023603 (2007).
- [9] S. Deng, G. Ortiz, and L. Viola, *Europhys. Lett.* **84**, 67008 (2008).
- [10] A. Polkovnikov, K. Sengupta, A. Silva, and M. Vengalattore, *Rev. Mod. Phys.* **83**, 863 (2011).
- [11] M. Kolodrubetz, B. K. Clark, and D. A. Huse, *Phys. Rev. Lett.* **109**, 015701 (2012).
- [12] T. Kibble, *J. Phys. A* **9**, 1387 (1976); W. H. Zurek, *Nature (London)* **317**, 505 (1985).

- [13] A. Polkovnikov, *Phys. Rev. B* **72**, 161201 (2005); C. De Grandi, V. Gritsev, and A. Polkovnikov, *ibid.* **81**, 012303 (2010).
- [14] R. H. Dicke, *Phys. Rev.* **93**, 99 (1954); H. Lipkin, N. Meshkov, and A. Glick, *Nucl. Phys.* **62**, 188 (1965).
- [15] A. Altland and V. Gurarie, *Phys. Rev. Lett.* **100**, 063602 (2008); A. Altland, V. Gurarie, T. Kriecherbauer, and A. Polkovnikov, *Phys. Rev. A* **79**, 042703 (2009).
- [16] T. Caneva, R. Fazio, and G. E. Santoro, *Phys. Rev. B* **78**, 104426 (2008).
- [17] V. M. Bastidas, C. Emary, B. Regler, and T. Brandes, *Phys. Rev. Lett.* **108**, 043003 (2012); G. Engelhardt, V. M. Bastidas, C. Emary, and T. Brandes, *Phys. Rev. E* **87**, 052110 (2013).
- [18] J. Reslen, L. Quiroga, and N. F. Johnson, *Europhys. Lett.* **69**, 8 (2005).
- [19] M. Greiner, O. Mandel, T. Esslinger, T. W. Hansch, and I. Bloch, *Nature (London)* **415**, 39 (2002).
- [20] I. Bloch, J. Dalibard, and W. Zwerger, *Rev. Mod. Phys.* **80**, 885 (2008).
- [21] A. Trabesinger, *Nat. Phys.* **8**, 263 (2012).
- [22] D. Porras and J. I. Cirac, *Phys. Rev. Lett.* **92**, 207901 (2004); K. Baumann, C. Guerlin, F. Brennecke, and T. Esslinger, *Nature (London)* **464**, 1301 (2010); J. Simon, W. S. Bakr, R. Ma, M. E. Tai, P. M. Preiss, and M. Greiner, *Nature (London)* **472**, 307 (2011).
- [23] S. Dusuel and J. Vidal, *Phys. Rev. Lett.* **93**, 237204 (2004).
- [24] C. Emary and T. Brandes, *Phys. Rev. Lett.* **90**, 044101 (2003).
- [25] See the Supplemental Material at <http://link.aps.org/supplemental/10.1103/PhysRevLett.112.030403> for details of the calculations and derivations.
- [26] A. Polkovnikov and V. Gritsev, *Nat. Phys.* **4**, 477 (2008).
- [27] A. Messiah, *Quantum Mechanics* (North Holland, Amsterdam, 1981), Vol. 2.
- [28] J. Vidal and S. Dusuel, *Europhys. Lett.* **74**, 817 (2006).
- [29] R. Botet, R. Jullien, and P. Pfeuty, *Phys. Rev. Lett.* **49**, 478 (1982); C. Emary and T. Brandes, *Phys. Rev. E* **67**, 066203 (2003).